Acta Physiologiae Plantarum (2018) 40:177
https://doi.org/10.1007/s11738-018-2751-3

ORIGINAL ARTICLE

Dehydration-induced changes in spectral reflectance indices and chlorophyll fluorescence of Antarctic lichens with different thallus color, and intrathalline photobiont

Barták Miloš[1] · Hájek Josef[1] · Morkusová Jana[1] · Skácelová Kateřina[1] · Košuthová Alica[2]

Received: 3 August 2017 / Revised: 27 August 2018 / Accepted: 28 August 2018 / Published online: 7 September 2018

Abstract

In this study, we investigated responses of the Photochemical Reflectance Index (PRI), and Normalized Difference Vegetation Index (NDVI) to gradual dehydration of several Antarctic lichen species (chlorolichens: *Xanthoria elegans, Rhizoplaca melanophthalma, Physconia muscigena*, cyanolichen: *Leptogium puberulum*), and a *Nostoc commune* colony from fully wet to a dry state. The gradual loss of physiological activity during dehydration was evaluated by chlorophyll fluorescence parameters. The experimental lichen species differed in thallus color, and intrathalline photobiont. In the species that did not exhibit color change with desiccation (*X. elegans*), NDVI and PRI were more or less constant (mean of 0.25, − 0.36, respectively) throughout a wide range of thallus hydration status showing a linear relation to relative water content (RWC). In contrast, the species with apparent species-specific color change during dehydration exhibited a curvilinear relation of NDVI and PRI to RWC. PRI decreased (*R. melanophthalma, L. puberulum*), increased (*N. commune*) or showed a polyphasic response (*P. muscigena*) with desiccation. Except for *X. elegans*, a curvilinear relation was found between the NDVI response to RWC in all species indicating the potential of combined ground research and remote sensing spectral data analyses in polar regions dominated by lichen flora. The chlorophyll fluorescence data recorded during dehydration (RWC decreased from 100 to 0%) revealed a polyphasic species-specific response of variable fluorescence measured at steady state—F_s, effective quantum yield of photosystem II (Φ_{PSII}), and non-photochemical quenching (qN). Full hydration caused an inhibition of Φ_{PSII} in *N. commune* while other species remained unaffected. The dehydration-dependent fall in Φ_{PSII} was species-specific, starting at an RWC range of 22–32%. Critical RWC for Φ_{PSII} was around 5–10%. Desiccation led to a species-specific polyphasic decrease in F_s and an increase in qN indicating the involvement of protective mechanisms in the chloroplastic apparatus of lichen photobionts and *N. commune* cells. In this study, the spectral reflectance and chlorophyll fluorescence data are discussed in relation to the potential of ecophysiological processes in Antarctic lichens, their resistance to desiccation and survival in Antarctic vegetation oases.

Keywords Spectral indices · PRI · NDVI · Non-photochemical quenching · James Ross Island

Introduction

Spectral reflectance indices are commonly used in plant physiology with numerous applications for higher plants (see e.g., Sun et al. 2014) and lichens (Bechtel et al. 2002). The main application is remote sensing in vegetation cover studies focused on the presence/absence of vegetation, species composition and water regime in plants. Recently, spectral features of lichens were studied mainly using airborne-based remote sensing (e.g., Zhang et al. 2005; Feng et al. 2013) so that it is now possible to distinguish between bare rock surfaces and lichen-dominated cover (Morison et al. 2014) in subpolar and polar regions. In this approach, spectral

---

Communicated by M. Horbowicz.

✉ Hájek Josef
jhajek@sci.muni.cz

[1] Laboratory of Photosynthetic Processes, Department of Experimental Biology, Faculty of Science, Masaryk University, University Campus-Bohunice, Kamenice 5, 62500 Brno, Czech Republic

[2] Department of Botany and Zoology, Faculty of Science, Masaryk University, University Campus-Bohunice, Kamenice 5, 62500 Brno, Czech Republic

reflectance curves are used typically to evaluate species-specific differences (Rees et al. 2004; Kiang et al. 2007). Recent technologies allow to distinguish particular lichen species by spectral patterns in near UV, visible and NIR as shown by Calviño-Cancela and Martín-Herrero (2016) in Antarctic vegetation oases. Within the last few decades, a new trend has appeared to study changes in spectral indices in relation to ongoing physiological processes using both field and laboratory-based measurements. Photosynthetic measurements using chlorophyll fluorescence have been taken in combination with spectral reflectance since it allows a non-invasive evaluation of the physiological status of a plant and analysis of its limiting factors (Perez-Priego et al. 2015). The Normalized Difference Vegetation Index (NDVI), and Photochemical Reflectance Index (PRI) are the most frequently used spectral indices both in controlled experiments and in the field. In higher plants, a decrease in NDVI is associated primarily with a decrease in chlorophyll contents (e.g., Chen and Chen 2008), water stress (Palumbo et al. 2008; Fabião et al. 2012) and the water regime (Yebra et al. 2013). However, a great variety of stressors has been studied using the NDVI approach ranging from leaf ageing (Letts et al. 2008), low light effects (Jiang et al. 2005), and salinity (Naumann et al. 2008) to ozone-caused damages to the leaf photosynthetic apparatus (Meroni et al. 2008). In lichens, NDVI has been used to assess the water status much less frequently than in higher plants, however, a variety of field and laboratory experimental set ups has been used to address different aspects of lichen ecophysiology. Gloser and Gloser (2007) reported a species-specific NDVI decrease with thallus dehydration. Garty et al. (2000) used NDVI as an early indicator of the negative effects of heavy metal impact on lichens, in particular their primary photosynthetic processes. Recently, NDVI was used in the vegetation mapping of several components (including lichens) of Antarctic vegetation oases at a few locations along the Antarctic Peninsula (Haselwimmer and Fretwell 2009).

The majority of reflectance indices are derived from the red and infrared wavelengths of the light spectrum. The PRI, however, exploits shorter wavelengths that are related to photosynthetic pigments, xanthophylls in particular. Specifically, reflectance at 531 nm is associated with the de-epoxidation state of xanthophyll cycle pigment, i.e., the violaxanthin to zeaxanthin conversion (Gamon et al. 1990; Gamon and Surfus 1999). Therefore, PRI is commonly used as an estimator of a short-term radiation and water stresses that generally activate zeaxanthin formation (e.g., Ripullone et al. 2011) and an increase in energy dependent- and non-photochemical quenching. The zeaxanthin-independent part of the non-photochemical quenching mechanisms, however, can not be detected by PRI (Fréchette et al. 2015). PRI, however, is also sensitive to actual photosynthetic pigment pool, the ratio of chlorophyll to carotenoids in particular, which is slowly changing and thus useful in long-term studies in higher plants (see, e.g., Gamon and Berry 2013). In cyanolichens, PRI is related to xanthophylls, since cyanobacteria do possess them (see Zakar et al. 2016 for review). They stabilize the structure of PSII. In *Nostoc commune*, which is a typical lichen-forming cyanobacterial species, apart from zeaxanthin which is reported for the species (Arima et al. 2012), the involvement of some special carotenoids, such as, e.g., β-cryptoxanthin, caloxanthin, and nostoxanthin (Takaichi et al. 2009 for *N. commune*) can not be excluded. Recently, Trnková and Barták (2017) reported dehydration-induced changes in PRI in Antarctic *Nostoc* sp. colonies.

PRI has recently been used as a good estimator of photosynthetic performance in leaves of higher plants (e.g., Trotter et al. 2002). That is why it is used in the studies exploiting simultaneous chlorophyll fluorescence parameters measurements (e.g., Guo and Trotter 2004). Several chlorophyll fluorescence parameters, effective quantum yield of PSII in particular (see e.g., Tubuxin et al. 2015) might be used for evaluation of photosynthesis. When scaled-up to the canopy level, PRI has a wide range of applications in the estimation of radiation use efficiency (RUE) of different ecosystems (Garbulsky et al. 2011), such as, e.g., grasslands (Balzarolo et al. 2015), evergreen conifers (Wong and Gamon 2015), Mediterranean vegetation dominated by a small broadleaf evergreen shrub (Stagakis et al. 2014), and a tropical evergreen forest (Nakaji et al. 2014).

Within the last decade, several attempts have been made to calculate the PRI and NDVI indices for lichen-dominated polar ecosystems using satellite data in vegetation mapping studies (Casanovas et al. 2015). A very promising approach for future studies in polar regions is using a combination of several techniques, composed of satellite spectral data, reference spectra of lichens (Harsanyi and Chang 1994), ground and laboratory studies focusing on the hydration dependence of PRI and NDVI (Barták et al. 2015a, b), made at the pixel and subpixel levels using satellite data. Moreover, increased application of satellite data analysis (Fretwell et al. 2011) and unmanned automatic vehicles will help to evaluate species patchiness in lichen-dominated small-area research plots more than the mid-resolution used typically in satellite imagery (Casanovas et al. 2015).

In lichens, the spectral reflectance and photosynthetic parameters of the thallus depend on actual hydration (Aubert et al. 2007). Interspecific differences accross a wide spectrum of species, however, exist depending mainly on the optical properties of a particular lichen, intrathalline content and composition of pigments and secondary metabolites. Our earlier studies conducted on autotrophs from polar regions showed dehydration-dependent changes in the spectral indices PRI and NDVI in *Umbilicaria* (Barták et al. 2015a) and colonies on non-lichenized *N. commune* (Trnková and Barták 2017). Since dehydration-induced changes in lichen spectral properties and the changes in photosynthetic performance happen simultaneously during thallus desiccation, simultaneous measurements of PRI, NDVI and chlorophyll fluorescence parameters related to the primary photochemical processes of photosynthesis are beneficial. The approach can evaluate the critical dehydration at which photochemical processes are limited and relate it to particular PRI and NDVI in different lichen species. Such an approach allows for relating the effective quantum yield of PS_{II} (Φ_{PSII}), which characterises the functioning of PS_{II} and consequent steps of photosynthetic linear electron transport in the thylakoid membranes of the chloroplast, to PRI, an indicator of the involvement of xanthophyll cycle pigments. PRI is, therefore, used as an estimator of protective non-photochemical processes activated in the chloroplastic apparatus of lichen symbiotic algae during desiccation. In our study, we studied chloro- and cyanolichens, and non-associated *N. commune*. The aim was to evaluate interspecific differences in PRI and NDVI changes in desiccating thalli. Such species-specific response of PRI and NDVI to dehydration would help to interpret spectral data for small-scale areas dominated by lichens in future studies. The objective of the study was to find species-specific differences in the two indices and relate the dehydration-induced changes in PRI and NDVI to different photobionts (alga/cyanobacteria), desiccation-induced decline in primary photosynthetic processes, and thallus optical properties, thallus color change from wet to dry state in particular. Last but not least, the aim of the study was to find the most sensitive spectral reflectance indices for particular species, i.e., those exhibiting the largest difference between wet and dry state.

Materials and methods

Sample collection and handling

Several lichen species from James Ross Island, Antarctica (Fig. 1) were used in the experiments: *Xanthoria elegans, Leptogium puberulum, Rhizoplaca melanophthalma, Physconia muscigena*, as well as a non-lichenized *N. commune* colony. The experimental species represent typical dominants of vegetation oases of the northern part of James Ross Island (Láska et al. 2011). The species samples were collected in February 2015 from deglaciated field sites: (1) a long-term research plot (63°48´03″S, 57°52´ 50″, see Barták et al. 2015a, b for details, *P. muscigena*), (2) a coastal terrace (63°48´10″S, 57°55´09″W, *R. melanophthalma*), and a deglaciated foothill of Berry Hill (63°48´51″S, 57°51´35″W, *L. puberulum, X. elegans*), see Fig. 1. After collection, the samples were delivered to the Czech Antarctic station Mendel, where the experiments were taken. Typically, ten samples sized at least 9 cm^2 (segments) were taken for each species for (1) spectral reflectance, and consecutive (2) chlorophyll fluorescence measurements. The experimental species differed in the color and optical properties of the upper thallus surface, and symbiotic intrathalline photosynthetizing partners (photobiont)—see species characteristics below.

Species characteristics

Xanthoria elegans is a foliose chlorolichen that has a unicellular green alga *Trebouxia* sp. as a photobiont. It forms typically flat lobate rosettes up to 6 cm wide or larger colonies over stone and soil surfaces. Thallus color is typically bright orange, however, some deep orange ecotypes could be found as well. The thallus possesses a variety of secondary metabolites such as, e.g., dominating parietin, and supplementary compounds such as fallacinal, emodin, teloschistin and parietinic acid. *X. elegans* is a cosmopolitan species colonizing various harsh habitats, including maritime and continental Antarctica (Øvstedal and Lewis Smith 2001). On James Ross Island, *X. elegans* grows on stony substrates well supplied by water, typically in shallow depressions or a microrelief with enhanced snow accumulation. *X. elegans* is tolerant to nitrogen (Munzi et al. 2012) and shows a high resistance to a variety of stressors such as, e.g., UV-B (Monteiro Estêvão 2015) and freezing temperatures (Barták et al. 2007).

Rhizoplaca melanophthalma is an umbilicate, *Trebouxia*-possessing chlorolichen with a polyphyllous, sometimes squamulose or pulvinate, thallus. Thallus color varies from usually light yellow to greenish yellow. When *R. melanophthalma* stays in a dry state for a long time in the field, the color may change to slightly brownish or grayish. Apothecia may form on a majority of the upper surface of the lichen. Since the apothecia color may vary from yellowish brown to black, the optical properties of the lichen differ to a large extent. For this reason, we involved two ecotypes of *R. melanophthalma* into this study: pale (with dominant yellow color and fewer apothecia), and black (with numerous black apothecia prevailing over the upper surface). Only a few studies have investigated the presence of secondary metabolites in the thallus. For example, Cansaran et al. (2006) reported usnic acid in *R. melanophthalma*.

Leptogium puberulum is a *Nostoc*-possessing cyanolichen thriving and photosynthesizing in long-term wet habitats such as temporal streams and seepages (Schlensog et al. 1997). It can, however, survive occasionally at places insufficiently supplied by liquid water thanks to its ability to hydrate from water vapor (Haranczyk et al. 2006). On James Ross Island, it occurs in similar habitats as *X. elegans*. The thallus of *L. puberulum* is blackish-brown to brownish-green, especially in the fully wet state. The upper and lower surfaces of the thallus are of the same

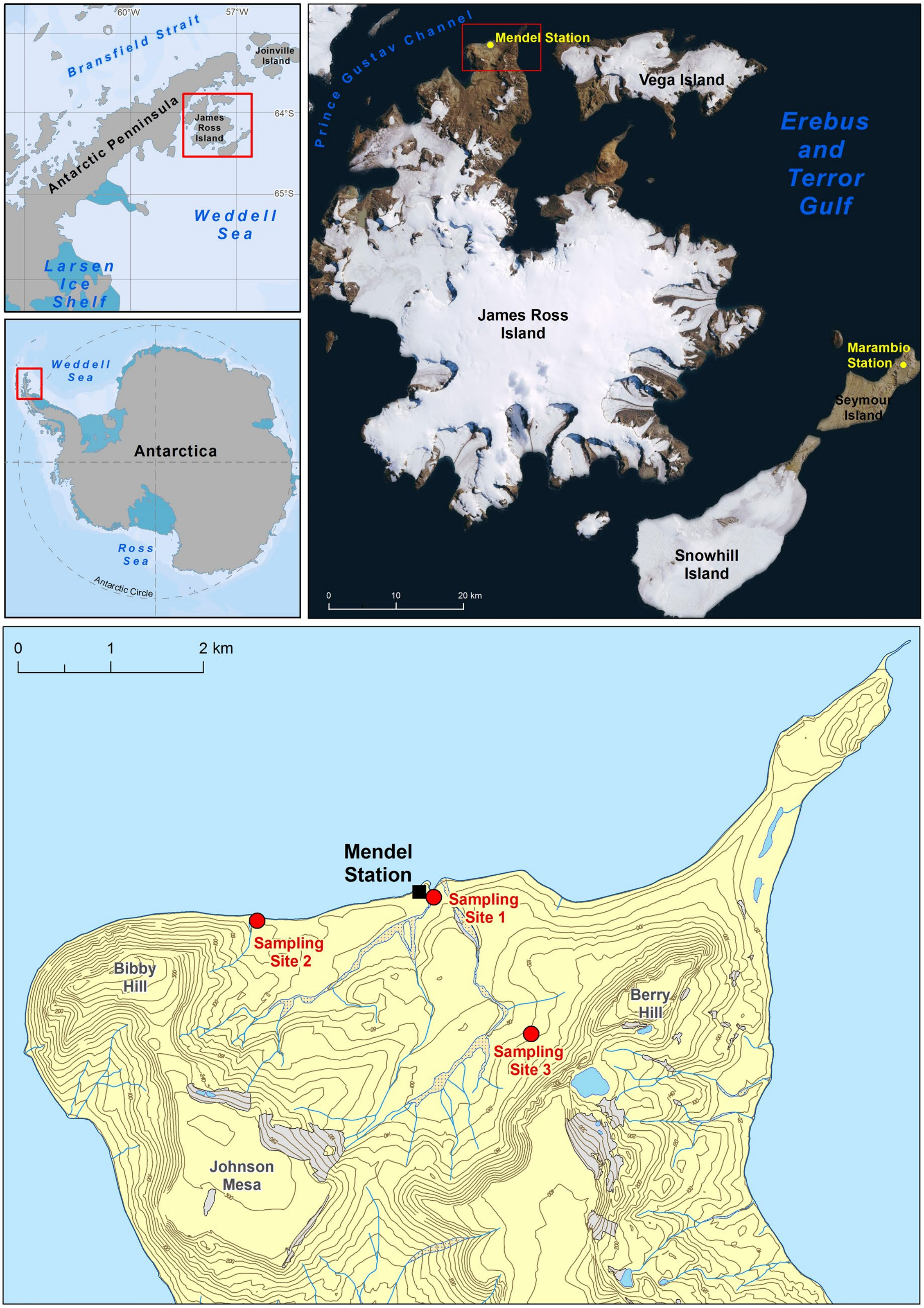
60°W
57°W
Bransfield Strait
Joinville Island
James Ross Island
64°S
Antarctic Penninsula
65°S
Weddell Sea
Larsen Ice Shelf
Weddell Sea
Antarctica
Ross Sea
Antarctic Circle
Prince Gustav Channel
Mendel Station
Vega Island
Erebus and Terror Gulf
James Ross Island
Marambio Station
Seymour Island
Snowhill Island
0
10
20 km
0
1
2 km
Mendel Station
Sampling Site 1
Sampling Site 2
Sampling Site 3
Bibby Hill
Berry Hill
Johnson Mesa

◂**Fig. 1** Map of James Ross Island (Antarctica) with indication of sampling sites of individual experimental species: *Physconia muscigena* (sampling site 1), *Rhizoplaca melanophthalma* (sampling site 2), *X. elegans, L. puberulum* (sampling site 3). Source: Czech Geological Survey. 2009. James Ross Island—northern part. Topographic map 1:25,000. First edition. Praha, Czech Geological Survey. ISBN 978-80-7075-734-5

color but the lower one is lighter. The thallus typically has numerous suberect to erect lobes forming a complex overlapping three-dimensional structure. UV-B absorbing compounds were detected in ethanol extracts with peak absorption at 202, 250 and 302 nm but these have yet to be identified in Antarctic *L. puberulum* samples (Barták et al. 2015b).

Physconia muscigena is a foliose *Trebouxia*-possessing chlorolichen quite common in maritime Antarctica (Øvstedal and Levis Smith 2001). It forms clusters up to 12 cm in diameter. Lobes are generally linear, 1–3 mm broad, usually ascending. The thallus of *P. muscigena* is pale gray-brown to dark brown. The upper surface might be lightly to heavily coated with pruina that disappear when the thallus gets wet and its color turns into a brighter green. On James Ross Island, *P. muscigena* is quite common in moist habitats (Block et al. 2009). Typically, it grows on the soil surface or over mosses. Its optical properties and secondary metabolites have been little studied, however, Kumar et al. (2014) reported phenolics, flavonoids and proanthocyanidins for the species while secalonic acid A (accessory pigment) and variolaric acid have also been reported for the species (LIAS database, http://liaslight.lias.net/).

Nostoc commune can be found in Antarctica in many terrestrial habitats as individual filaments encapsulated in exopolysaccharidic envelopes. The filaments are composed of numerous vegetative cells and N-fixing thick-walled heterocysts. Alternatively, *N. commune* forms large sheet-like colonies up to several hundreds of square centimeters. These are found as crusts when dry and inactive, but rapidly change to gelatinous physiologically active jelly-like structures when wet (e.g., Novis et al. 2007). In Antarctica, *N. commune* colonies thrives well in water-supplied microhabitats such as, e.g., shallow ponds, streams and seepages as reported from several Antarctic regions including the Antarctic Peninsula (Broady 1996), and James Ross Island (Komárek et al. 2015). *N. commune* is highly resistant to many environmental stress factors, such as, e.g., extreme temperature (Sand-Jensen and Jespersen 2012), UV-radiation (Ehling-Schulz and Scherer 1999; Monteiro Estêvão 2015), freeze–thaw cycles (Gupta 2011) and dehydration. On James Ross Island, *N. commune* colonies are formed mainly in seepages and represent a substantial component of the vegetation cover of long-term research plots established in such a habitat (Barták and Váczi 2014).

RWC of lichen thalli during dehydration

The thalli segments of individual species were placed on a wet disk of paper on the bottom of Petri dishes and hydrated in closed dishes. The segments were sprayed by demineralized water regularly each 6 h for 24 h. Fully hydrated thalli segments (i.e., those exhibiting maximum individual weight after 24 h—tested on laboratory scales) were depried of water droplets remaining on thallus surface by a blotting paper gently and than used for measurements. Measurements of spectral reflectance indices and photosynthetic measurements were done in ten samples for each species desiccating from a fully hydrated to a fully dry state. On each sample, a single measurement was done (i.e., 10 measurements = replicates). During the desiccation, room temperature was kept constant (18 °C, 40% RH) and the lichen thalli were left in open Petri dishes to desiccate naturally. Relative water content (RWC) was gravimetrically evaluated before spectral measurements. Samples were weighed on an AS 310 analytical scale (RADWAG, Poland), and RWC calculated according to the equation:

$$\mathrm{RWC}\,(\%) = [(F_\mathrm{m} - D_\mathrm{m})/(W_\mathrm{m} - D_\mathrm{m})] \times 100, \quad (1)$$

where F_m is the actual fresh mass (weight) of a sample, D_m is the mass of the fully dry sample (oven-dried sample at 35 °C for 24 h), and W_m, is the mass of the fully wet sample.

NDVI and PRI measurements

NDVI and PRI of the lichen thalli segments were measured repeatedly during gradual dehydration from fully wet (RWC = 100%) to dry (RWC = 0–10%) states. The NDVI was measured by a PlantPen NDVI 300 (Photon System Instruments, Czech Republic) while the PRI was measured by a PlantPen PRI 200 (Photon System Instruments, Czech Republic). Both instruments use a particular spectral reflectance for calculation of the indices using the following equations:

$$\mathrm{NDVI} = (R_{740} - R_{660})/(R_{740} + R_{660}), \quad (2)$$

$$\mathrm{PRI} = (R_{570} - R_{531})/(R_{570} + R_{531}). \quad (3)$$

Chlorophyll fluorescence

Chlorophyll fluorescence parameters were measured independently on PRI, and NDVI measurements. On light-acclimated samples (segments of thallus, area of about 4 cm^2), variable chlorophyll fluorescence (F_s), effective quantum yield of photochemical processes in PSII (Φ_PSII), and non-photochemical quenching (qN) were measured in response to RWC when the samples were desiccated from a fully hydrated to dry state. In this study, variable fluorescence is understood as the chlorophyll fluorescence signal induced by a light incident on desiccating lichen samples. Therefore, it is sensu stricto a steady state fluorescence emitted from a light-adapted sample, and thus abbreviated F_s. Samples were let to dry at room temperature (25 °C) with RH of 70% (measured by a HOBO datalogger, OnSet Computers, USA) under moderate light (60 µmol m^{-2} s^{-1} of photosynthetically active radiation). According to the sample dimension/weight and complexity of the thallus structure, dehydration time varied between 10 and 18 h. During that time, sample weight and chlorophyll fluorescence parameters were measured repeatedly every 5 min. A Mettler scale (Mettler AE-100, Germany) and a fluorometer (PAM 2000, H. Walz, Germany) were used for these purposes. Variable chlorophyll fluorescence at steady state—F_s was measured by a fluorometer. Effective quantum yield of the photochemical processes of photosynthesis in photosystem II (Φ_{PSII}), and non-photochemical quenching (qN) were calculated from measured data by routine procedures as described earlier in Barták et al. (2004) and expressed as dependent on RWC. Particular chlorophyll fluorescence parameters were calculated as:

$$\Phi_{\mathrm{PSII}} = (F'_{\mathrm{m}} - F_{\mathrm{s}})/F'_{\mathrm{m}}, \tag{4}$$

$$\mathrm{qN} = (F_{\mathrm{m}} - F'_{\mathrm{m}})/(F_{\mathrm{m}} - F_{\mathrm{o}}), \tag{5}$$

where F_m is the maximum chlorophyll fluorescence recorded on a dark-adapted sample (5 min) after application of a saturation pulse, F'_m is the maximum chlorophyll fluorescence recorded on a light-adapted sample after application of a saturation pulse, F_s is the steady state fluorescence in a light-adapted sample, and F_o is the minimum chlorophyll fluorescence. Chlorophyll fluorescence parameters were plotted against RWC for each parameter and experimental species. Then, the RWCs at which the chlorophyll fluorescence parameters showed changes were evaluated. These were RWCs at which (a) the first sign of decline (F_s, Φ_{PSII}) or increase (qN) was apparent and (b) a parameter equaled to zero (critical RWC). Three different phases were found in the F_s/Φ_{PSII}/qN to RWC relationships: (1) phase I at high hydration associated with suprasaturation effect, (2) phase II found in a wide range of RWCs typical by a linear increase/decrease of particular parameter with ongoing dehydration, and (3) phase III found typically at the RWC fall from 30 to 0%. The phase III exhibited a typical *S* curve of particular parameter.

Spectral reflectance

Reflectance spectra were measured on leaf size-scale in dry and wet thalli of the experimental lichen species. Before measurements on wet lichens, the thalli were rehydrated in between two wet sheets of papers placed in a Petri dishes for 24 h. During the wetting period, thalli were placed into a fridge (5 °C) and exposed to a dim light (10 µmol m^{-2} s^{-1} of photosynthetically active radiation). For the leaf size-scale measurements, a PolyPen RP 400 spectral reflectometer (Photon Systems Instruments, Czech Republic) was used. The instrument measured within a wavelength range from 320 to 800 nm with sampling interval of 2 nm. For each species and the treatment (wet/dry), at least six spectra were measured and mean spectrum calculated. From the spectral curves, the following spectral indices were calculated: Greeness index (GI), Modified Chlorophyll Absorption in Reflectance Index (MCARI), Transformed CAR Index (TCARI), Normalized Phaeophytinization Index (NPQI), and Structure Intensive Pigment Index (SIPI)—see Table 1 for equations. Hydration-dependent differences in the above-listed spectral

Table 1 List of spectral reflectance indices used in this study for wet and dry thalli of experimental lichen species *P. muscigena, R. melanophthalma, X. elegans, L. puberulum*, and colony of *N. commune*

Index specification (abbreviations)/equation	Source
Greeness Index (*G*) $G = R_{554}/R_{677}$	Smith et al. (1995)
Modified Chlorophyll Absorption in Reflectance Index (MCARI) $\mathrm{MCARI} = [(R_{700} - R_{670}) - 0.2 \times (R_{700} - R550)] \times (R_{700}/R_{670})$	Daughtry et al. (2000)
Transformed CAR Index (TCARI) $\mathrm{TSARI} = 3 \times [(R_{700} - R_{670}) - 0.2 \times (R_{700} - R_{550}) \times (R_{700}/R_{670})]$	Haboudane et al. (2002)
Normalized Phaeophytinization Index (NPQI) $\mathrm{NPQI} - (R_{415} - R_{435})/(R_{415} + R_{435})$	Barnes et al. (1992)
Structure Intensive Pigment Index (SIPI) $\mathrm{SIPI} - (R_{790} - R_{450})/(R_{790} + R_{650})$	Penuelas et al. (1995)

Greeness Index, MCARI and TCARI are parameters of chlorophyll contents and most sensitive indicators of vigorous growth and effective productivity. NPQI is a typical stress indicator evaluating phaeophytinization, i.e., degradation of chlorophyll molecules phaeophytin, a pigment involved into charge separation in photosystem II. Phaeophytization is responsible for a blueshift in the pigment spectrum of lichens. SIPI is typically attributed to nutritional status and photosynthetic pigments contents (typically carotenoid to chlorophyll a ratio). Recently, SIPI is, similarly to PRI, considered an indicator of effective photosynthetic processes reflectance indices were calculated as a difference between dry and wet values for particular species. Consequently, species-specific effects of hydration on the shape of the spectral curves and spectral reflectance indices were evaluated and discussed.

Statistical analysis

For spectral indices, species-specific differences and the differences related to hydration status (wet/dry) were analyzed using an ANOVA (STATISTICA v. 13, Dell Inc.), the LSD test in particular.

Results

PRI declined with progressive dehydration from fully wet (RWC = 100%) to a dry state (RWC = 0%) in a majority of the studied species. *N. commune* and *P. muscigena*, however, showed a slight increase and a biphasic response (a decrease followed by an increase) with dehydration, respectively. The PRI dehydration-response curves (Fig. 2) differed in their shapes as well as the range of PRI values reached during dehydration. A linear relation was found in *X. elegans* (Fig. 2a) and *R. melanophthalma* (Fig. 2c—pale ecotype). PRI changed only a little throughout the whole RWC range in *X. elegans* (− 0.3 to − 0.4), while the relation was much steeper in *R. melanophthalma* reaching PRI values within the range of 0 to − 0.1. Moreover, the black *R. melanophthalma* ecotype (Fig. 2d) showed somewhat higher PRI values than the pale one (mean difference 0.016). In contrast to this expectation, the shapes of the PRI to RWC curves did not differ much between the cyano- and chlorolichens. The only difference was that, apart from the shape of the relation, the PRI values were found to be somewhat higher (even positive) in *N. commune* (− 0.04 to 0.02) and *L. puberulum* (− 0.12 to − 0.04)—see Fig. 2b and e, respectively. In *L. puberulum*, a PRI response curve was apparent in the desiccating sample which showed more or less no PRI change within the RWC range of 30–100%. With pronounced thallus dehydration (RWC declining from 30 to 0%), PRI decreased exponentially. The minimum PRI value of − 0.14 was found in the fully desiccated *L. puberulum* thallus. In *N. commune*, PRI responded to dehydration within a narrow range (− 0.05 to 0.02) showing a curvilinear increase in PRI with increasing RWC, in contrast to *Nostoc*-possessing *L. puberulum*. The *P. muscigena* dehydration-response curve showed a somewhat complex curvilinear PRI to RWC relationship. PRI declined in the RWC range of 75–100% until the minimum of about − 0.15, then it rose with dehydration (RWC decline from 75 to 10%). PRI then remained more or less constant reaching a value of − 0.06 under severe thallus dehydration (RWC 0–10%). In general, *P. muscigena* showed PRI within the range of − 0.04 to − 0.15 (Fig. 2f). The PRI values decreased at the initial phase of dehydration (RWC decline from 100 to 75%). Then, PRI increased with further dehydration (RWC decline from 75 to 0%).

NDVI to RWC relationship was curvilinear in majority of the studied species (Fig. 3). In *X. elegans*, however, the relationship was linear (Fig. 3a). The observed linear relationship showed a slight increase in NDVI with dehydration. The thallus did not show any visible change in color remaining bright orange in all stages of dehydration. Other species showed curvilinear responses of NDVI with maximum values found at the RWCs ranging within 20–50% (Fig. 3, B, C, D, and E, respectively). For *N. commune, R. melanophthalma*—both pale and black ecotype, and *L. puberulum*, NDVI increased from fully wet (RWC = 100%) to a partially dehydrated state reaching species-specific maxima at 20 (*R. melanophthalma*—pale ecotype, Fig. 3c), 30 (*R.melanophthalma*—black ecotype, Fig. 3d, L. *puberulum*, Fig. 3e), and 50% RWC (*N. commune*, Fig. 3b). *P. muscigena* (Fig. 3f) showed rather constant NDVI values within the RWC range of 50–100%. With dehydration from the RWC of 50–0%, it declined in a curvilinear manner.

In all studied species, F_s exhibited a biphasic course with desiccation (Fig. 4). Phase I was typified by a constant-rate gradual decrease in F_s from fully (RWC = 100%) to a partially dehydrated state (typically 30–40% RWC). Then, a much faster decline in F_s followed in phase II, occurring with a decrease in RWC from 30 to 5%. In all species, phase II led to an *S*-curve relationship of F_s to RWC. Phase I, however, differed interspecifically in the rate of F_s decline with RWC fall. It was slow in *P. muscigena, R. melanophthalma*, and *L. puberulum* resulting in shallow decline, in contrast to the much steeper F_s decline recorded in *N. commune*. F_s decreased linearly in *R. melanophthalma* with decreasing RWC from 100 to 30%. Then, F_s decreased rapidly with further dehydration (RWC from 30 to 5%), showing an *S*-curve relation, and reached zero at 5% RWC. Similarly, *L. puberulum* showed two phases of F_s decrease with dehydration.

Maximum Φ_{PSII} values were found at the full hydration state (RWC = 100%) for a majority of the species (see, e.g., *P. muscigena*, Fig. 5). *N. commune*, however, showed a water suprasaturation effect resulting in decreased Φ_{PSII} (to about 60% of maximum) at full hydration (RWC within 80–100%, denoted as phase I hereafter). Surprisingly, *L. puberulum* possessing *Nostoc* sp. as the photosynthesizing partner, had a different dehydration-response curve with a typical more or less constant increase in Φ_{PSII} when RWC decreased from 100 to 25% (phase II), followed by a decrease in the RWC range of 25–0%. A suprasaturation effect on Φ_{PSII} was also apparent in the chlorolichen *P. muscigena*, however, the Φ_{PSII} inhibition was found only in a very limited extent (100–95% of RWC) of hydration (phase I). In *N. commune*, an increase in Φ_{PSII} was found with further dehydration

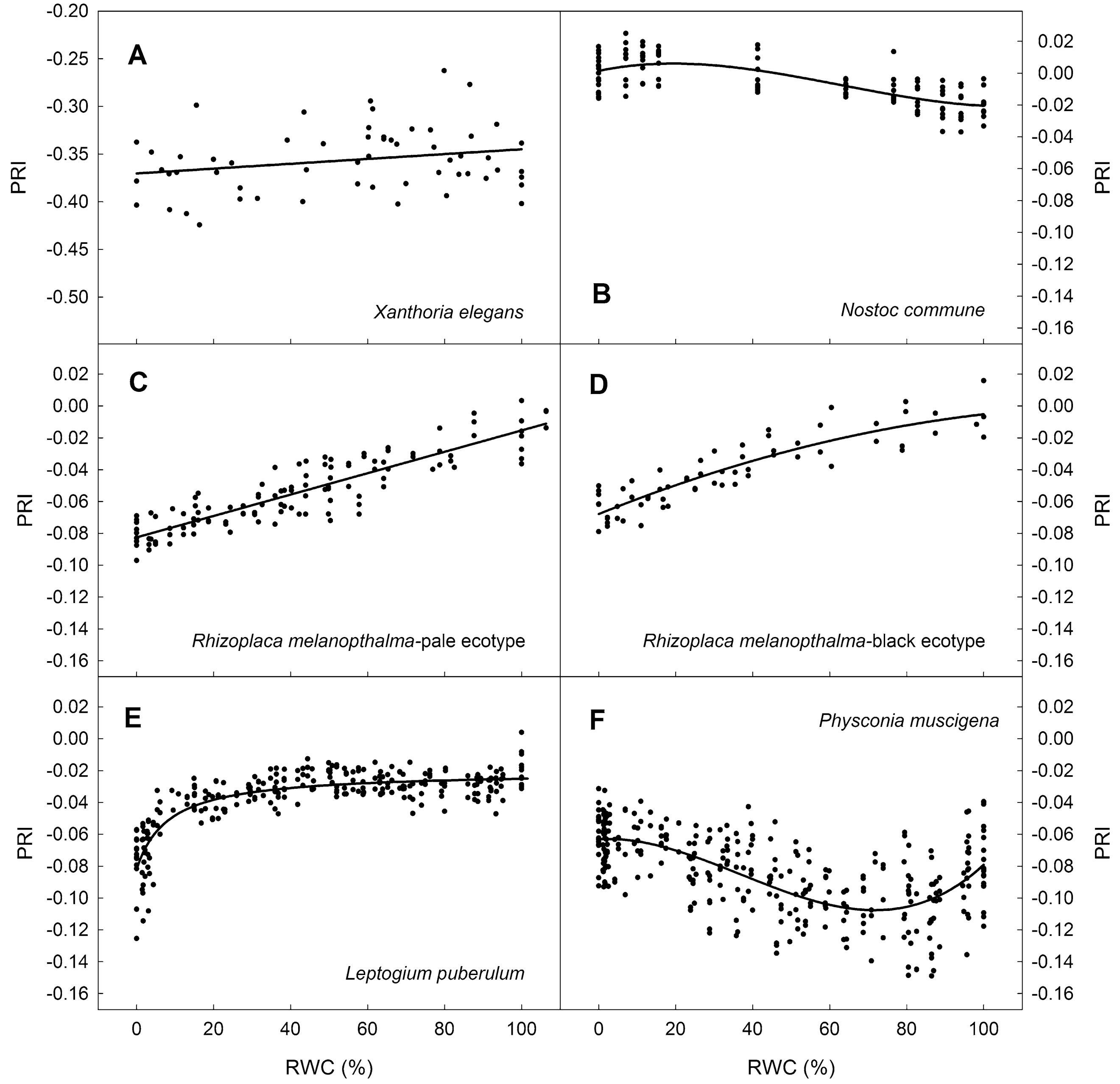

Fig. 2 Courses of Photochemical Reflectance Index (PRI) of experimental species in response to relative water content (RWC) recorded during gradual dehydration from fully wet (RWC-100%) to dry state (RWC = 0%). *X. elegans* (**a**), *N. commune* (**b**), *R. melanophthalma*—pale ecotype (**c**), *R. melanophthalma*—black ecotype (**d**), *L. puberulum* (**e**), *P. muscigena* (**f**). Data points and best-fit line/curves are presented. Equations: **a** ($y = 3\times10^{-4}\times x - 0.3703$, $R^2 = 0.2312$), **b** ($y = 8.1798\times10^{-8}\times x^3 - 1.5421\times10^{-5}\times x^2 + 5\times10^{-4}\times x + 0.0014$, $R^2 = 0.7252$), **c** ($y = 7\times10^{-4}\times x - 0.0825$, $R^2 = 0.8996$), **d** ($y = -3.4729\times10^{-6}\times x^2 + 10^{-3}\times x - 0.0679$, $R^2 = 0.8973$), **e** ($y = 0.0616\times x/(8.1889 + x) - 0.0821$, $R^2 = 0.8423$), **f** ($y = 2.6847\times10^{-7}\times x - 2.979\times10^{-5}\times x + 10^{-4}\times x - 0.0631$, $R^2 = 0.6366$)

of the colony (RWC decrease from 80 to 30%, phase II). Maximum Φ_{PSII} was reached at a RWC of 30% followed by a consequent decline with further dehydration (phase III, RWC below 30%). Critical RWC, at which Φ_{PSII} reached 0, was found at 5% in *N. commune*. In *R. melanophthalma*, and *P. muscigena*, Φ_{PSII} remained constant and even slightly increased within a wide range of decreasing RWC values (from 100 to 24% RWC), however, further dehydration led to a rapid *S*-curve decrease in Φ_{PSII} followed by full Φ_{PSII} inhibition at a RWC of 5%.

Non-photochemical quenching (qN, Fig. 6) increased linearly with desiccation from 100 to 30% RWC. With more pronounced dehydration (RWC decrease from 30 to 5% RWC), qN increased to a maximum of 1. Such a biphasic

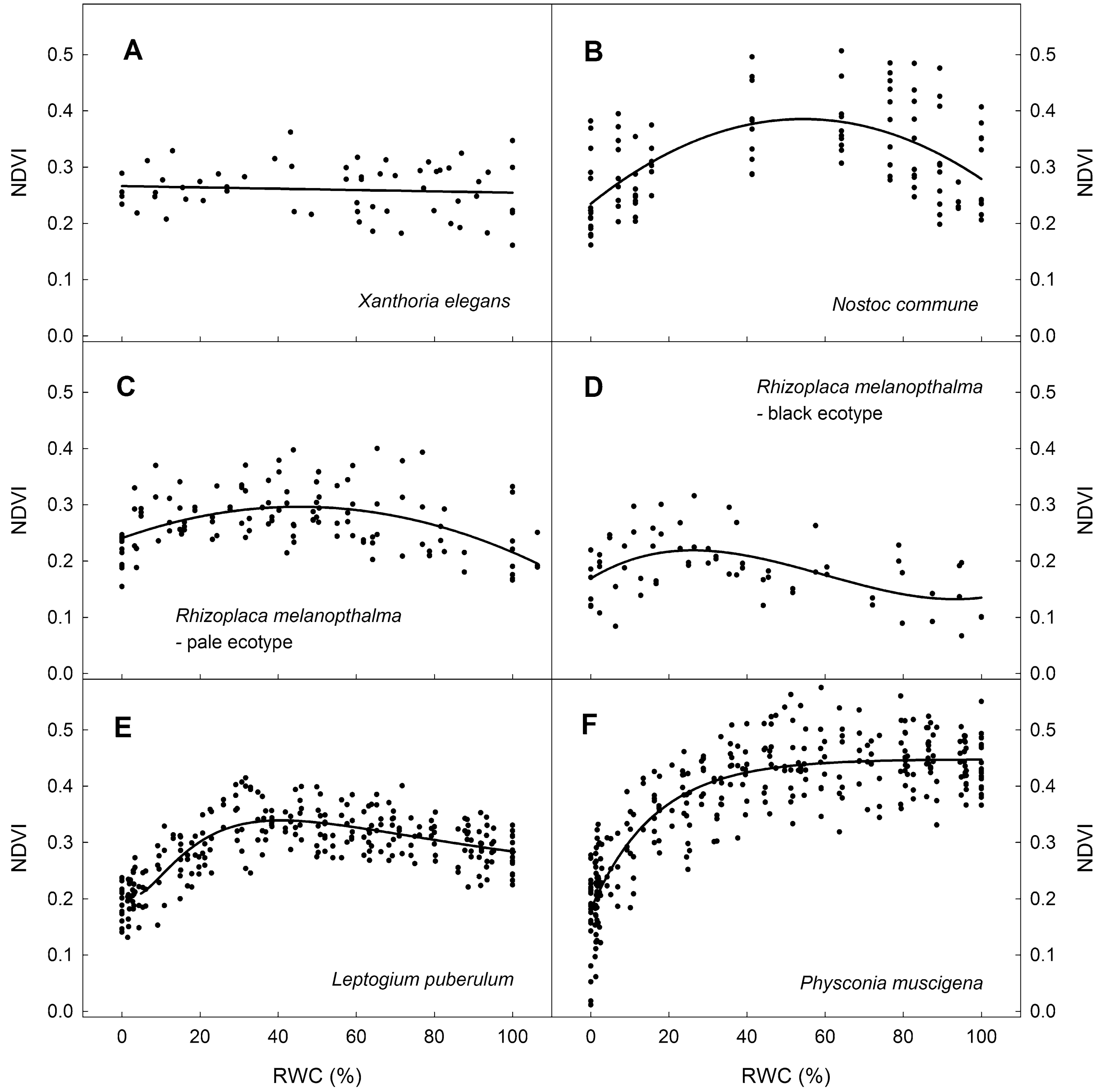

Fig. 3 Courses of Normalized Difference Vegetation Index (NDVI) of experimental species in response to relative water content (RWC) recorded during gradual dehydration from fully wet (RWC-100%) to dry state (RWC = 0%). *X. elegans* (**a**), *N. commune* (**b**), *R. melanophthalma*—pale ecotype (**c**), *R. melanophthalma*—black ecotype (**d**), *L. puberulum* (**e**), *P. muscigena* (**f**). Data points and best-fit line/curves are presented. Equations: **a** ($y=-10^{-4}\times x+0.2662$, $R^2=0.0842$), **b** ($y=-5.1052\times 10^{-5}\times x^2+5.5\times 10^{-3}\times x+0.2348$, $R^2=0.5756$), **c** ($y=-2.7118\times 10^{-5}\times x^2+2.5\times 10^{-3}\times x+0.2407$, $R^2=0.4896$), **d** ($y=5.7573\times 10^{-7}\times x^3-10^{-4}\times x^2+0.0042\times x+0.169$, $R^2=0.5257$), **e** ($y=\exp(-0.5\times(\ln(x/89.7022)/0.8883)^2)/x)+0.2011$, $R^2=0.7915$), **f** ($y=0.1151\times(1-\exp(-0.0608\times \mathrm{x}))+0.1526\times(1-\exp(-0.0608\times x))+0.1804$, $R^2=0.8704$)

response was, however, species-specific. In phase I (RWC decline from 100 to 30–40%), a small increase in qN was apparent in *P. muscigena, R. melanophthalma*, and *N. commune*, while no increase was found in *L. puberulum*. Phase II, with further decline in RWC from 20/30–0%, was typified by a more or less S-shaped increase of qN to the maximum value. Interspecific differences were apparent in terms of the RWCs at which qN equaled 0. It was reached at 8% RWC in *N. commune*, while more pronounced desiccation was necessary for *R. melanophthalma* (2%), and *L. puberulum* (5%).

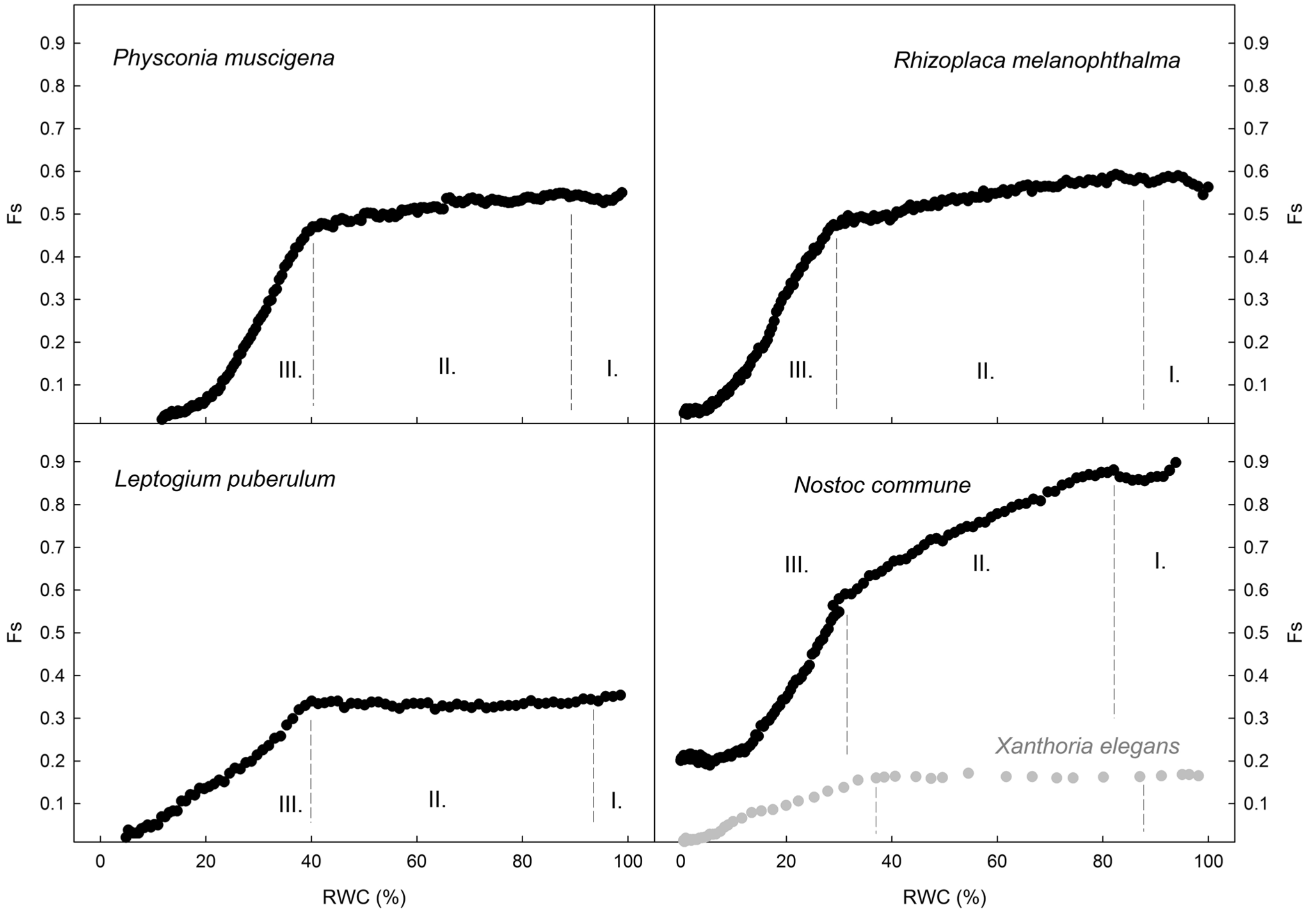

Fig. 4 Relation of a steady state chlorophyll fluorescence (F_s) to RWC during dehydration (RWC from 100 to 0%) for individual species. Phases I (RWC from 80/90 to 100%), II (RWC 30/40–80/90%), and III (RWC from 0 to 30/40%), respectively, with different slopes can be distinguised. Data points represent pooled data of three replicates. Standard deviations of the F_s mean calculated for the RWC classes (100–97%, …,3–0% RWC, data not shown) are below 8% (phase I), 6% (phase II), and 9% (phase III) of the mean for all the species

Spectral reflectance curves

For a single species, spectral reflectance curves differed in dry and wet state of lichen thallus (see Fig. 7). In the chlorolichen *P. muscigena*, the reflectance values were found higher in dry state. The highest difference was found at the wavelength of 530 nm. In *X. elegans* and *R. melanophthalma* (pale ecotype), however, both increased and decreased spectral reflectance values were found in wet state: (1) increased within the ranges of 380–580 nm, and 700–780 nm, (2) decreased within the range of 580–700 nm. In the cyanolichen *L. puberulum*, spectral reflectance curve was found rather flat. The reflectance values slightly increased within the range of 400–680 nm. Then, the rate of increase was higher in the range of 680–800 nm. The spectral curves, however, showed no difference between dry and wet thalli. Colonies of the cyanobacterium *N. commune* showed very similar shape of the spectral reflectance curves. The spectral reflectance curve recorded in wet state, however, showed somewhat higher values then the curve recorded in dry state.

Spectral indices derived from the curves are presented in Table 2. The highest relative change in numerical value of the particular indices recorded for dry and wet state was found for *X. elegans* (Greeness index: 44.8%, MCARI 93.3%), *P. muscigena* (TCARI − 157.4%, SIPI 41.2%), and *N. commune* (− 187.4%).

Discussion

The PRI to RWC relationships produced species-specific curves. The differences might be attributed to the differences in photosynthetizing pigments in chlorolichens (possessing *Trebouxia* sp.) and cyanolichens. Chlorolichens, their symbiotic algae in particular, possess xanthophyll cycle pigments, the involvement of which (zeaxanthin formation) is reported in dehydration responses in lichens (Kranner et al. 2003,

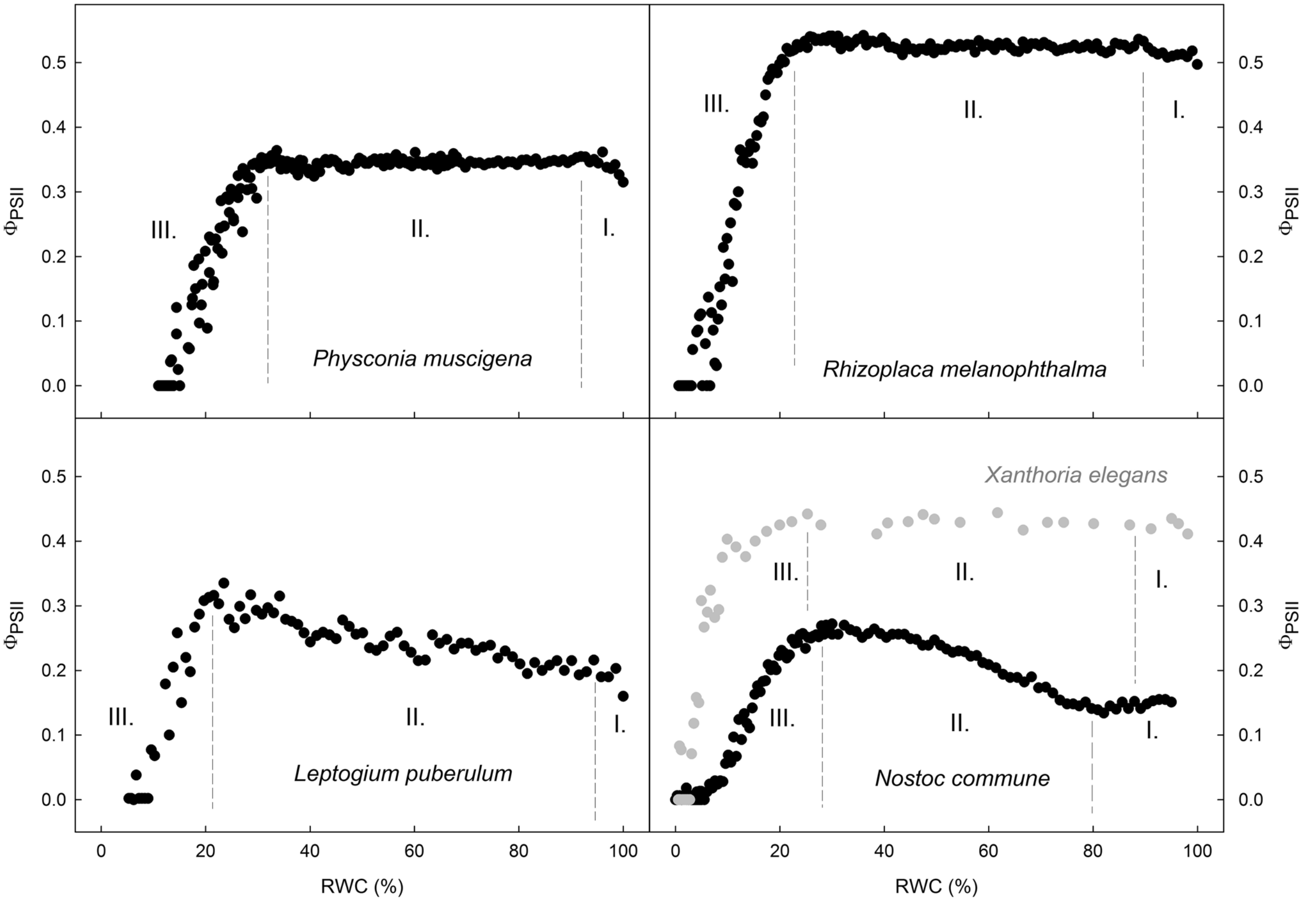

Fig. 5 Relation of effective quantum yield of photochemical processes in photosystem II (Φ_{PSII}) to RWC during dehydration (RWC from 100 to 0%) for individual species. Phases I (attributed to hypersaturation effect), II, and III, respectively, with different slopes can be distinguised. Data points represent pooled data of three replicates. Standard deviations of the Φ_{PSII} mean calculated for the RWC classes (100–97%, …,3–0% RWC, data not shown) are below 9% (phase I), 9% (phase II), and 10% (phase III) of the mean for all the species

2005). Some cyanobacteria, *N. commune* specifically, have either a reduced xanthophyll cycle pool or lack it completely which negatively affects the PRI, which is generally attributed to the violaxanthin to zeaxanthin conversion. Since *L. puberulum* has a cyanobacterium as its photosynthesizing partner, the PRI to RWC relation in this species and *N. commune* should differ from those measured in chlorolichens.

Data from earlier studies done on lichens from polar regions (Jupa et al. 2012; Barták et al. 2015a, b), however, support the idea that a majority of chlorolichens shows negative PRI within a wide range of thallus desiccation. Other lichen species, however, may exhibit positive PRI values and a decreasing trend with thallus dehydration (*Stereocaulon foliosum*, Singh et al. 2013, *Parmelia* sp.; Gates et al. 1965). Therefore, no general response of PRI to thallus dehydration in lichens can be postulated. Moreover, optical properties of the upper cortex, its changes during dehydration in particular may play a role as suggested by Orekhova et al. (2018). The study reported the changes in NDVI, PRI related to presence/absence of the upper cortex in particular lichens. Removal of the upper cortex led to a 10% increase in NDVI values within the whole range of RWC in desiccating thalli (RWC from 100 to 0%). Shapes of the curves in NDVI to RWC relationship were generally the same for particular species as shown in Fig. 3, however, some species showed a decrease in NDVI in a higher RWC (*Leptogium puberulum*: 83%, *P. muscigena*: 51%—Orekhova et al. 2018) than in our study. The upper cortex removal led to a slight decrease in PRI values, the PRI to RWC relationship, however, remained unaffected.

NDVI decreases exponentially with thallus dehydration, as reported by Gloser and Gloser (2007) for lichens and for the lichen components forming soil crusts in a cold desert in China (Yamano et al. 2006). Similarly, Singh et al. (2013) reported NDVI decrease when comparing data measured at 93 and 37% of RWC. Our data, however, indicate a slight, species-specific decrease in NDVI at full (RWC = 100%) and close-to-full hydration. The decrease could be related to the possibility that the maximum NDVI of the lichen thalli in our study occurred at a hydration status that was less than

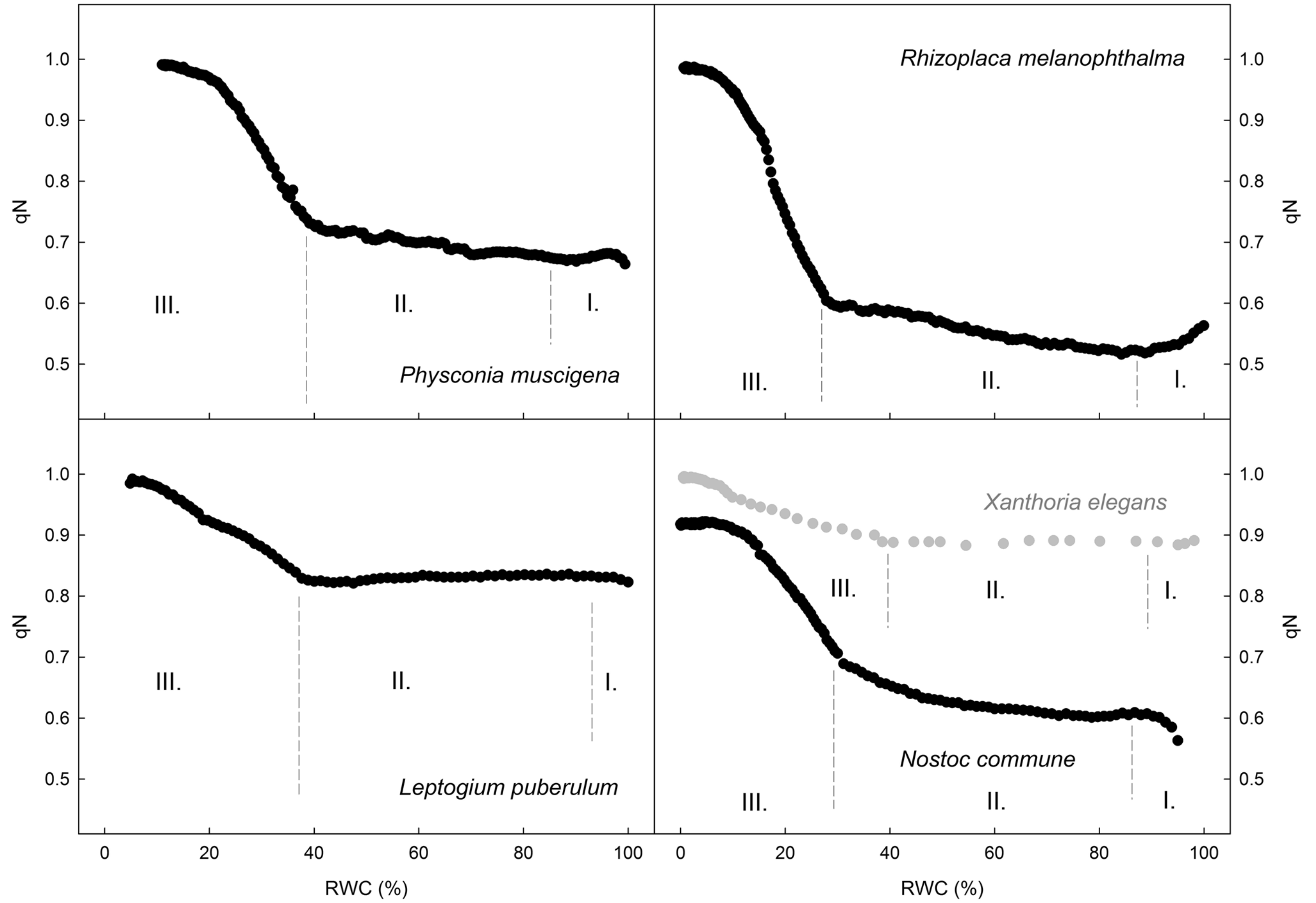

Fig. 6 Dehydration-dependent activation of non-photochemical quenching (qN) during RWC decrease from 100 to 0% for individual species. Typically, the phases I (90–100% RWC), II (30/40–90% RWC), and III (0–30/40% RWC), can be distinguised. qN to RWC relationship tends to be generally linear in phase II, and following a *S*-curve in the phase III of dehydration. Standard deviations of the qN mean calculated for the RWC classes (100–97%, …,3–0% RWC, data not shown) are below 6% (phase I), 5% (phase II), and 9% (phase III) of the mean for all the species

full hydration, but a level that was not necessarily used in the above-mentioned studies. Generally, decreasing NDVI was found with progressive thalli dehydration (RWC falling from 30 to 0%) in all species except *X. elegans* which showed almost constant NDVI for the desiccating thallus, and a very limited range of values (0.2–0.3), see Fig. 3. Species specificity of NDVI in response to desiccation is most likely due to different optical properties of the desiccating thallus. Barták et al. (2015a, b) reported species-specific rates of NDVI decrease in three lichen species with contrasting thallus color in the sequence: green (*Umbilicaria arctica*)—reddish brown (*Stereocaulon foliosum*)—brownish-black (*Umbilicaria hyperborea*).

The change in F_s decline rate found during desiccation at the RWCs of 30–40% could be attributed to the early stage of dehydration stress on primary photosynthetic processes since Φ_{PSII} and qN started to decrease (Φ_{PSII}), and increase (qN) at the same RWC. In all the studied species, there was an S-shaped decline of F_s at the RWC range from 0 to 30/40%, which might be attributed to a gradual loss of water from the photobiont cells and a consequent decrease in the chlorophyll fluorescence signal (Lange et al. 1989). Some studies report desiccation-induced decrease in Fo thanks to the changes in the optical properties of the lichen cortex (Gauslaa and Solhaug 2001), and increased non-radiative dissipation of absorbed excitation energy (Komura et al. 2010; Wieners et al. 2012). Desiccation-induced involvement of non-radiative dissipation is demonstrated as the increase in non-photochemical quenching (qN) found in all species studied (see Fig. 6). Such an increase in qN is a well described phenomenon in lichen photobionts documenting the involvement of zeaxanthin formation (e.g., Fernández-Marín et al. 2010), increased contents of antioxidants (e.g., Kranner et al. 2005), conformational changes of pigment–protein complexes, and thermal dissipation of absorbed light energy (Heber 2008), dehydration-induced PSII deactivation (e.g., Kosugi et al. 2009), and xanthophyll cycle-independent mechanisms (Veerman et al. 2007) which

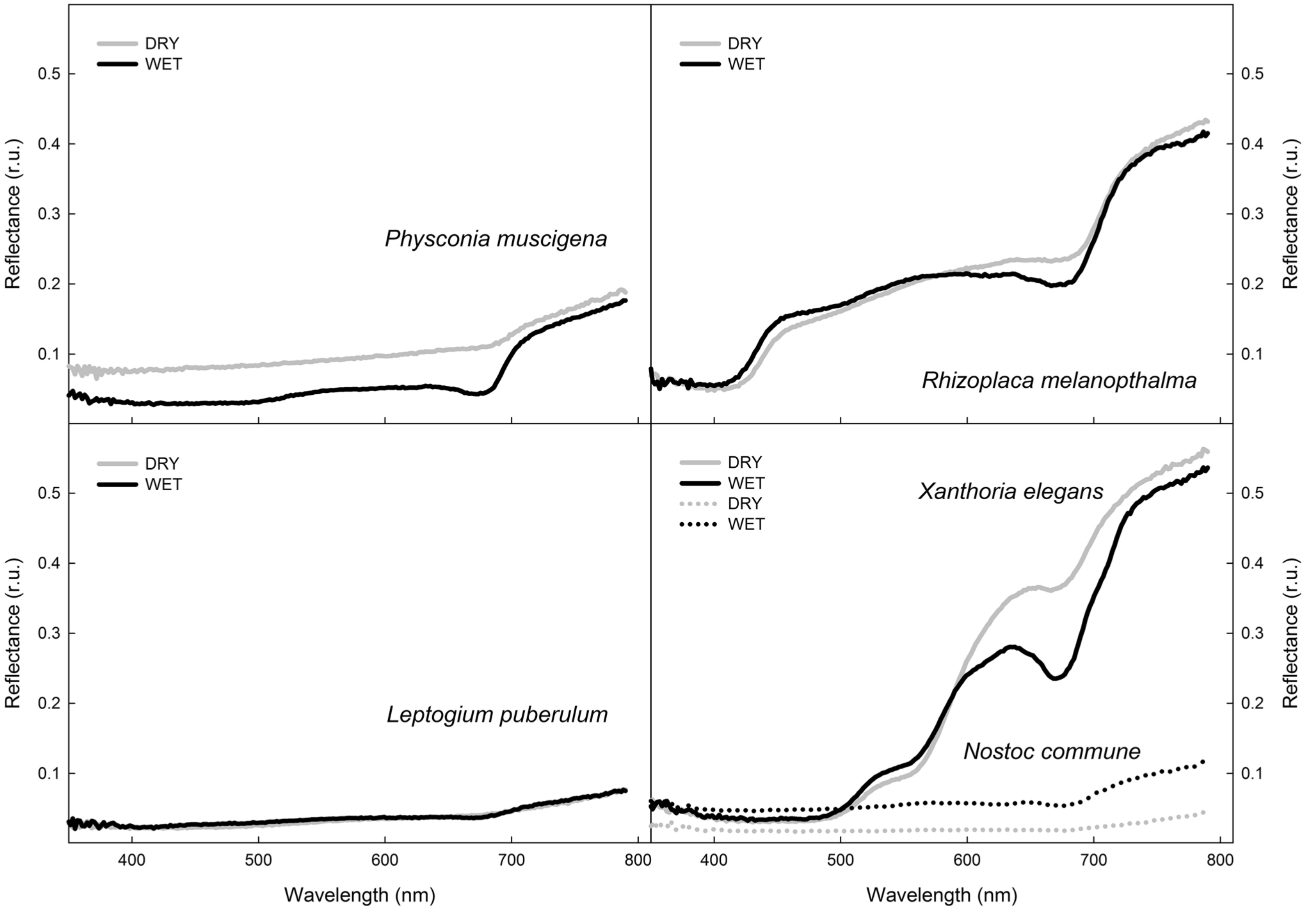

Fig. 7 Spectral reflectance curves recorded for dry and wet thalli of chlorolichens (*P. muscigena, R. melanophthalma*, and *X. elegans*), cyanolichen (*L. puberulum*), and *N. commune* colony. The spectra were recorded within the wavelength range of 380–790 nm. The spectra are means of at least five replicates

is attributed to chlorophyll molecules aggregation in light harvesting complexes of PSII or a new type of quenching in PSII core antenna (Komura et al. 2010). These mechanisms protect PSII from the damage caused by the desiccation-induced PSII overenergization and formation of reactive oxygen species. These mechanisms, however, can not completely prevent PSII damage caused by light during desiccation. Therefore, continuous metabolic repair is required to compensate for such damage. In lichens and other desiccation-tolerant photoautotrophs during desiccation, ultra-fast energy dissipation is activated (Heber et al. 2010; Heber 2012) as a part of qN. Recently, two mechanisms are considered for chlorophyll fluorescence quenching in desiccating lichens (Slavov et al. 2013): (1) direct quenching of the PSII, (2) absorbed energy transfer from PSII to PSI (spillover). The latter mechanism is considered more efficient in *Trebouxia*-possessing chlorolichen *Parmelia sulcata* (Slavov et al. 2013). Thus, the strong relationship between F_s and qN as found in our data ($P < 0.001$) for all the studied lichen species indicates the effective involvement of qN during desiccation. Similarly to lichens (e.g., Veerman et al. 2007), a highly effective drought-induced non-photochemical quenching (designated d-NPQ) was decribed recently in mosses and found stronger than that caused by PSII charge separation or non-photochemical quenching (NPQ)—Yamawaka and Itoh (2013). In our experimental design, numerical values of qN recorded in dry state (RWC range of about 0–20%) might be overestimated due to the fact, that a decrease in F'_m (see Eq. 5 for qN calculation) is not attributed to desiccation-induced quenching exclusively. Part of F'_m decrease is related to the changes in optical properties (reduced transmittance) of the upper cortex. In this way, light amount reaching the photobiont layer in desiccated thalli was less than that in fully hydrated thalli (RWC = 100%). Such phenomenon is well documented in desiccating lichens (Büdel and Lange 1994; Gauslaa and Solhaug 2001). It is, however, species-specific.

The effective quantum yield of PSII in chlorolichens (*P. muscigena, R. melanophthalma*) showed a typical *S* curve at the RWC range from 22 to 0% RWC, as was demonstrated

Table 2 Spectral reflectance indices recorded for dry and wet thalli of the experimental lichen species (*P. muscigena, R. melanopthalma, L.puberulum, X. elegans*) and the colony of *N. commune*

Index		*Physconia muscigena*		*Rhizoplaca melanopthalma*		*Leptogium puberulum*		*Xanthoria elegans*		*Nostoc commune*	
		Mean	Std	Mean	Std	Mean	Std	Mean	Std	Mean	Std
Greeness Index											
Dry		0.8114^{cd}	±0.0404	0.8476^{cd}	±0.0513	0.8024^{c}	±0.0502	0.2640^{a}	±0.0191	1.0286^{f}	±0.0458
Wet		1.0932^{f}	±0.1621	1.0415^{ef}	±0.0585	0.9264^{de}	±0.0778	0.4781^{b}	±0.0908	1.0629^{f}	±0.0933
MCARI											
Dry		0.0136^{a}	±0.0027	0.0348^{ab}	±0.0164	0.0033^{a}	±0.0021	0.0072^{a}	±0.0186	0.0039^{a}	±0.0030
Wet		0.1102^{d}	±0.0512	0.0701^{bc}	±0.0242	0.0110^{a}	±0.0068	0.1079^{cd}	±0.0567	0.0177^{a}	±0.0112
TCARI											
Dry		-0.0976^{d}	±0.0328	-0.2068^{f}	±0.0300	-0.0360^{ab}	±0.0120	-0.1633^{e}	±0.0346	-0.0185^{a}	±0.0070
Wet		-0.0383^{ab}	±0.0156	-0.1805^{ef}	±0.0202	-0.0322^{ab}	±0.0118	-0.0716^{cd}	±0.0215	-0.0514^{bc}	±0.0153
NPQI											
Dry		0.0080^{bc}	±0.0064	-0.2312^{a}	±0.0265	0.0216^{c}	±0.0658	0.0435^{c}	±0.0200	0.0394^{c}	±0.0520
Wet		0.0038^{bc}	±0.0343	-0.2790^{a}	±0.0316	-0.0331^{b}	±0.0709	0.0367^{c}	±0.0418	0.0137^{bc}	±0.0170
SIPI											
Dry		0.3682^{ab}	±0.0819	0.4576^{c}	±0.0528	0.4424^{bc}	±0.0342	0.5666^{d}	±0.0154	0.3838^{a}	±0.0326
Wet		0.6266^{d}	±0.0474	0.4220^{abc}	±0.0657	0.4094^{abc}	±0.0624	0.6178^{d}	±0.0322	0.3667^{a}	±0.0837
(Wet − dry) × 100/wet	GI	25.8		18.6		13.4		44.8		3.2	
	MCARI	87.6		50.4		69.7		93.3		77.8	
Relative change (%)	TCARI	−154.7		−14.6		−12.0		−127.9		64.0	
	NPQI	−107.1		17.1		165.3		−18.5		−187.4	
	SIPI	41.2		−8.4		−8.1		8.3		−4.7	

Presented data are means of at least five measurements and standard deviations. The letters in the upper index indicate statistically significant differences related to the species and hydration status (dry/wet). For calculations of the differences ($P = 0.05$), ANOVA (LSD test) was used. Key to the abbreviations: GI—Greenness Index, MCARI—Modified Chlorophyll Absorption in Reflectance Index, TCARI—Transformed CAR index, NPQI—Normalized Phaeophytinization Index, and SIPI—Structure Intensive Pigment Index for a variety of lichens (Barták 2014; Barták et al. 2015a, b). Similarly, data form an earlier study (Nayaka and Saxena 2014) indicated that the rapid decline in potential photochemical reactions in PSII (Fv/Fm) was lessened at RWCs below 20%. In contrast, the dehydration-response curve of Φ_{PSII} in the *N. commune* colony had a polyphasic character with 2 or 3 main phases (Fig. 5). At the RWC range of 80–100% RWC (phase I), Φ_{PSII} was more or less constant (0.15) and related to the reduction of the diffusive flux of dissolved inorganic carbon to the colony thanks to boundary layer thickness (Sand-Jensen 2014). With further desiccation, phases II (Φ_{PSII} increase) and III (S-shaped Φ_{PSII} decrease) were distinguished and, similarly to Barták et al. (2016), attributed to an increased supply of CO_2 into the colony due to reduced resistance to gas exchange and dehydration-induced limitation of primary photosynthetic processes, respectively.

Response curves of PRI nd NDVI (Figs. 2, 3) had different shape than those of F_s, Φ_{PSII}, and qN (Figs. 4, 5, 6). In some species, however, changes in PRI corresponded to the changes in qN. This is particularly valid for *N. commune*. Whenever qN reached maximum at RWC of 15%, PRI reached its maximum and remained constant with further dehydration. Similarly to previous study (Trnková and Barták 2017), optimum RWC for NDVI was 50%. The NDVI values could be affected by phycocynine present in *N. commune* cells (Shukia et al. 2008) since the spectral reflectances between 610 and 650 nm are included into phycocynine index (see, e.g., Kutser et al. 2006).

In *L. puberulum*, PRI started to decline at RWCs below 20%, which coincidences with the ´turning point´ of Φ_{PSII} which started to decline at this RWC as well. Since the other species did not show any of the above-described phenomenon, it is not easy to interpret. Some of the studied species, e.g., *X. elegans*, and *R. melanophthalma* do not show any relation of PRI to F_s, Φ_{PSII}, and qN. Therefore, some follow-up studies are to be done to substantiate the relation of PRI/NDVI to chlorophyll fluorescence parameters in lichens.

Reflectance spectra recorded for individual lichen species and colonies of *N. commune* showed hydration-depended changes. Generally, higher reflectance values were found for dry chlorolichens compared to wet state spectra. *X. elegans* showed a remarkably different spectral reflectance, typical by a high reflectance at the wavelengths range of 500–800 nm associated with its bright-colored orange pigments (Van Der Veen and Csatho 2005). It is caused by parietin that have a high reflectance in the ranges of 600–680 and above 740 nm (Gauslaa and Ustvedt 2003, c.f. also Fig. 7). Parietin is typically located in the top layer of the upper cortex in a form of tiny extracellular crystals (Honegger 1990). Parietin shows seasonality with the highest values recorded in summer (Gauslaa and McEvoy 2005). In dry *X. elegans* thalli with crystalic parietin, the reflectance seems to be higher then in wet thalli. Similarly, *R. melanophthalma* exhibited high spectral reflectance values in the range of 530–800 nm which might be related to a high contents of extracellular yellow pigments, usnic and pulvinic acids in particular (Piovano et al. 1997). The yellow usnic acid is one of the most common lichen substances having an absorption in 220 and 290 nm (Huneck and Yoshimura 1996). Strong reflectance of usnic acid is reported by Nelson et al. (2013) for *Cladonia stellaris* in the ranges 520–600, 620–680, and above 720 nm (c.f. Fig. 7, *R. melanophthalma*). Therefore, usnic acid might be responsible for the reflectance increase in the range of 450–600 nm and above 720 nm (see Fig. 7). Pulvinic acid, has an absorption ain 256 and 347–357 nm (Huneck and Yoshimura 1996; Hauck et al. 2009). For pulvinic acid derivates, absorption at 405–412 nm is reported (Huang et al. 2009). Surprisingly, data on pulvinic acids reflectance are not available, however, reflectance in the range of 500–700 might be expected. Reflectance spectra for dark-pigmented *P. muscigena, L. puberulum*, and *N. commune* were similar to those reported by Bechtel et al. (2002). The spectra, however, did not show an increase of spectral reflectance at about 750 nm as reported by Gloser and Gloser (2007) for dark-pigmented *Umbilicaria hirsuta*. The increase is typical rather for the lichens that posses green or green-brownish color of thallus as demonstrated by, e.g., Rees et al. (2004) and Singh et al. (2013). In all species, a minimum at about 660–675 nm was found in wet thalli which relates to the chlorophyll absorption maxima at 662 and 642 nm.

The spectral reflectance indices (Table 2) showed that they differed to a large extent in wet and dry lichen thalli. SIPI (expressing the ratio between carotenoids and chlorophylls) showed a big difference in *P. muscigena*, which demonstrate a change from brownish-black color in dry state to bright green when the thallus is wet. NPQI proved to have an indicative value in desiccating lichens since it showed more than 100% change between dry and wet state in majority of the tested lichens. In conclusion, all the tested indices showed a substantial difference between dry and wet state. In follow-up studies focused on lichens, therefore, we suggest to measure the spectral reflectance indices (GI, MCARI, TCARI, NPQI, SIPI and possibly the other indices) in response to RWC, so that they could be related to either primary photosynthetic processes (Φ_{PSII} in particular) during dehydration or protective mechanisms activated in photosynthetic apparatus of photobionts, qN in particular. Such approach has a great potential for future field-based ecophysiological studies in lichen-dominated Arctic and Antarctic ecosystems. Recently, similar studies exploiting vegetation spectral indices and LANDSAT data are done in cryptogamic cover in South African drylands exhibiting different hydration within a growing season (Rodriguez-Caballero et al. 2016).

Author contribution statement Contribution of the authors of the paper was as follows: (1) Idea of the project: MB, (2) Experimentation: MB, JH, JM, KS, AK, (3) Data interpretation: MB, JH, JM, (4) Manuscript writing: MB, JH, JM, KS.

Acknowledgements The authors thank the projects CzechPolar-I, II (LM2010009 and LM2015078) for providing field facilities in Antarctica and the infrastructure for the research reported in this study. The authors thank also for the support from ECOPOLARIS project (CZ.02.1.01/0.0/0.0/16_013/0001708).

References

Arima H, Horiguchi N, Takaichi S, Kofuji R, Ishida K-I, Wada K, Sakamoto T (2012) Molecular genetic and chemotaxonomic characterization of the terrestrial cyanobacterium *Nostoc commune* and its neighboring species. FEMS Microbiol Ecol 79:34–45

Aubert S, Juge C, Boisson AM, Gout E, Bligny R (2007) Metabolic processes sustaining the reviviscence of lichen *Xanthoria elegans* (Link) in high mountain environments. Planta 226:1287–1297

Balzarolo M, Vescovo L, Hammerle A, Gianelle D, Papale D, Tomelleri E, Wohlfahrt G (2015) On the relationship between ecosystem-scale hyperspectral reflectance and CO_2 exchange in European mountain grasslands. Biogeosciences 12:3089–3108

Barnes JD, Balaguer L, Manrique E, Elvira S, Davison AW (1992) A reappraisal of the use of DMSO for the extraction and determination of chlorophylls a and b in lichens and higher plants. Environ Exp Bot 32:85–100

Barták M (2014) Lichen photosynthesis. Scaling from the cellular to the organism level. In: Hohmann-Marriot MF (ed) The structural basis of biological energy generation. Advances in photosynthesis and respiration. Springer, Dordrecht, pp 379–400

Barták M, Váczi P (2014) Long-term fluorometric measurements of photosynthetic processes in Antarctic moss *Bryum* sp. during austral summer season. Czech Polar Rep 4:63–72

Barták M, Hájek J, Vráblíková H, Dubová J (2004) High-light stress and photoprotection in *Umbilicaria antarctica* monitored by chlorophyll fluorescence imaging and changes in zeaxanthin and glutathione. Plant Biol 6:333–341

Barták M, Váczi P, Hájek J, Smykla J (2007) Low temperature limitation of primary photosynthetic processes in Antarctic lichens *Umbilicaria antarctica* and *Xanthoria elegans*. Polar Biol 31:47–51

Barták M, Trnková K, Hansen ES, Hazdrová J, Skácelová K, Hájek J, Forbelská M (2015a) Effect of dehydration on spectral reflectance and photosynthetic efficiency in *Umbilicaria arctica* and *U. hyperborea*. Biol Plant 59:357–365

Barták M, Hazdrová J, Jáchymová G, Pláteníková E, Monteiro Estevao DM, Hájek J, Skácelová K, Váczi P, Balarinová K (2015b) Photosynthetic parameters and synthesis of UV-B absorbing compounds is species-specific in Antarctic lichens exposed to supplemental UV-B radiation. In: 14. ČSEBR conference, Brno, Czech Republic, 2015. Bulletin ČSEBR, p 69. ISSN 1213-6670

Barták M, Hazdrová J, Skácelová K, Hájek J (2016) Dehydration-induced responses of primary photosynthetic processes and spectral reflectance indices in Antarctic *Nostoc* sp. Czech Polar Rep 6:87–95

Bechtel R, Rivard R, Sanchez-Azofeifa A (2002) Spectral properties of foliose and crustose lichens based on laboratory experiments. Remote Sens Environ 82:389–396

Block W, Lewis Smith RI, Kennedy AD (2009) Strategies of survival and resource exploitation in the Antarctic fellfield ekosystem. Biol Rev 84:449–484

Broady PA (1996) Diversity, distribution and dispersal of Antarctic terrestrial algae. Biodivers Conserv 5:1307–1335

Büdel B, Lange OL (1994) The role of cortical and epinecral layers in the lichen genus *Peltula*. Cryptogam Bot 4:262–269

Calviño-Cancela M, Martín-Herrero J (2016) Spectral discrimination of vegetation classes in ice-free areas of Antarctica. Remote Sens 8:856

Cansaran D, Cetin D, Halici MG, Atakol O (2006) Determination of usnic acid in some *Rhizoplaca* species from Middle Anatolia and their antimicrobial activities. Z Naturforsch C 61:47–51

Casanovas P, Black M, Fretwell P, Convey P (2015) Mapping lichen distribution on the Antarctic Peninsula using remote sensing, lichen spectra and photographic documentation by citizen scientists. Polar Res 34:25633

Chen J-C, Chen C-T (2008) Correlation analysis between indices of tree leaf spectral reflectance and chlorophyll content. In: Proceedings. The international archives of the photogrammetry, remote sensing and spatial information sciences. Part B7. Beijing, vol XXXVII, pp 231–238

Daughtry CST, Walthall CL, Kim MS, Brown de Colstoun E, McMurtrey JE III (2000) Estimating corn leaf chlorophyll concentration from leaf and canopy reflectance. Remote Sens Environ 74:229–239

Ehling-Schulz M, Scherer S (1999) UV protection in cyanobacteria. Eur J Phycol 34:329–338

Fabião M, Ferreira MI, Conceição N, Silvestre J (2012) Transpiration and water stress effects on water use, in relation to estimations from NDVI: application in a vineyard in SE Portugal. In: Erena M, López-Francos A, Montesinos S, Berthoumieu J-P (eds) The use of remote sensing and geographic information systems for irrigation management in southwest Europe, Zaragoza, pp 203–208

Feng J, Rivard B, Rogge D, Sánchez-Azofeifa A (2013) The longwave infrared (3–14 μm) spectral properties of rock encrusting lichens based on laboratory spectra and airborne SEBASS imagery. Remote Sens Environ 131:173–181

Fernández-Marín B, Becerril JM, García-Plazaolaeri JI (2010) Unravelling the roles of desiccation-induced xanthophyll cycle activity in darkness: a case study in *Lobaria pulmonaria*. Planta 231:1335–1342

Fréchette E, Wong CYS, Junker LV, Chang Ch-Y, Ensminger I (2015) Zeaxanthin-independent energy quenching and alternative electron sinks cause a decoupling of the relationship between the Photochemical Reflectance Index (PRI) and photosynthesis in an evergreen conifer during spring. J Exp Bot 66:7309–7323

Fretwell PT, Convey P, Fleming AH, Peat HJ, Hughes KA (2011) Detecting and mapping vegetation distribution on the Antarctic Peninsula from remote sensing data. Polar Biol 34:273–281

Gamon JA, Berry JA (2013) Facultative and constitutive pigment effects on the Photochemical Reflectance Index (PRI) in sun and shade conifer needles. Isr J Plant Sci 60:85–95

Gamon JA, Surfus JS (1999) Assessing leaf pigment content and activity with a reflectometer. New Phytol 143:105–117

Gamon JA, Field CB, Bilger W, Björkman O, Fredeen A, Peñuelas J (1990) Remote sensing of the xanthophyll cycle and chlorophyll fluorescence in sunflower leaves and canopies. Oecologia 85:1–7

Garbulsky MF, Penuelas J, Gamon J, Inoue Y, Filella I (2011) The photochemical reflectance index (PRI) and the remote sensing of leaf, canopy and ecosystem radiation use efficiencies: a review and meta-analysis. Remote Sens Environ 115:281–297

Garty J, Weissman L, Tamir O, Beer S, Cohen Y, Karnieli A, Orlovsky L (2000) Comparison of five physiological parameters to assess the vitality of the lichen *Ramalina lacera* exposed to air pollution. Physiol Plant 109:410–418

Gates DM, Keegan HJ, Schleter JC, Weidner VR (1965) Spectral properties of plants. Appl Opt 4:11–20

Gauslaa Y, McEvoy M (2005) Seasonal changes in solar radiation drive acclimation of the sun-screening compound parietin in the lichen *Xanthoria parietina*. Basic Appl Ecol 27:75–82

Gauslaa Y, Solhaug K-A (2001) Fungal melanins as a sun screen for symbiotic green algae in the lichen *Lobaria pulmonaria*. Oecologia 126:462–471

Gauslaa Y, Ustvedt EM (2003) Is parietin a UV-B or a blue-light screening pigment in the lichen *Xanthoria parietina*? Photochem Photobiol Sci 2:424–432

Gloser J, Gloser V (2007) Changes in spectral reflectance of a foliar lichen *Umbilicaria hirsuta* during desiccation. Biol Plant 51:395–398

Guo JM, Trotter CM (2004) Estimating photosynthetic light-use efficiency using the photochemical reflectance index: variations among species. Funct Plant Biol 31:255–265

Gupta RK (2011) Freeze recovery and nitrogenase activity in Antarctic cyanobacterium *Nostoc commune*. In: International conference on nanotechnology and biosensors IPCBEE, vol 25. IACSIT Press, Singapore, pp 116–124

Haboudane D, John R, Millera JR, Tremblay N, ZarcoTejada PJ, Dextraze L (2002) Integrated narrow-band vegetation indices for prediction of crop chlorophyll content for application to precision agriculture. Remote Sens Environ 81:416–426

Haranczyk H, Bacior M, Jastrzebska P, Olech MA (2006) Deep dehydration of Antarctic lichen *Leptogium puberulum* Hue observed by NMR and sorption isotherm. Acta Phys Pol A 115:516–520

Harsanyi JC, Chang Ch-I (1994) Hyperspectral image classification and dimensionality reduction: an orthogonal subspace projection approach. IEEE Trans Geosci Remote Sens 32:779–785

Haselwimmer C, Fretwell P (2009) Field reflectance spectroscopy of sparse vegetation cover on the Antarctic peninsula. In: First workshop on hyperspectral image and signal processing: evolution in remote sensing. Grenoble, France. https://doi.org/10.1109/WHISPERS.2009.5289099

Hauck M, Willenbruch K, Leuschner Ch (2009) Lichen substances prevent lichens from nutrient deficiency. J Chem Ecol 35(1):71–73

Heber U (2008) Photoprotection of green plants: a mechanism of ultrafast thermal energy dissipation in desiccated lichens. Planta 228:641–650

Heber U (2012) Conservation and dissipation of light energy in desiccation-tolerant photoautotrophs, two sides of the same coin. Photosynth Res 113:5–13

Heber U, Bilger W, Türk R, Lange OL (2010) Photoprotection of reaction centres in photosynthetic organisms: mechanisms of thermal energy dissipation in desiccated thalli of the lichen *Lobaria pulmonaria*. New Phytol 185:459–470

Honegger R (1990) Mycobiont–photobiont interactions in adult thalli and in axenically resynthesized pre-thallus stages of *Xanthoria parietina* (Teloschistales, lichenized Ascomycetes). Bibl Lichenol 38:191–208

Huang Y-T, Onose Y-I, Abe N, Yoshikawa K (2009) In vitro inhibitory effects of pulvinic acid derivates isolated from Chinese edible mushrooms, *Boletus calopus* and *Suillus bovinus*, on cytochrome P450 activity. Biosci Biotechnol Biochem 73:855–860

Huneck S, Yoshimura I (1996) Idetification of lichen substances. Springer, Berlin

Jiang Y, Carrow RN, Duncan RR (2005) Physiological acclimation of seashore paspalum and bermudagrass to low light. Sci Hort 105:101–115

Jupa R, Hájek J, Hazdrová J, Barták M (2012) Interspecific differences in photosynthetic efficiency and spectral reflectance in two *Umbilicaria* species from Svalbard during controlled desiccation. Czech Polar Rep 2:31–41

Kiang NY, Siefert J, Govindjee, Blankenship RE (2007) Spectral signatures of photosynthesis. I. Rev Earth Org Astrobiol 7:222–251

Komárek J, Genuario DB, Fiore MF, Elster J (2015) Heterocytous cyanobacteria of the Ulu Peninsula, James Ross Island, Antarctica. Polar Biol 38:475–492

Komura M, Yamagishi A, Shibata Y, Iwasaki I, Itoh S (2010) Mechanism of strong quenching of photosystem II chlorophyll fluorescence under drought stress in a lichen, *Physciella melanchla*, studied by subpicosecond fluorescence spectroscopy. Biochim Biophys Acta 1797:331–338

Kosugi M, Maiko Arita M, Shizuma R, Moriyama Y, Kashino Y, Koike H, Satoh K (2009) Responses to desiccation stress in lichens are different from those in their photobionts. Plant Cell Physiol 50:879–888

Kranner I, Zorn M, Turk B, Wornik S, Beckett RP, Batič F (2003) Biochemical traits of lichens differing in relative desiccation tolerance. New Phytol 160:167–176

Kranner I, Cram WJ, Zorn M, Wornik S, Yoshimura I, Stabentheiner E, Pfeifhofer HW (2005) Antioxidants and photoprotection in a lichen as compared with its isolated symbiotic partners. PNAS 102:3141–3146

Kumar J, Dhar P, Tayade AB, Gupta D, Chaurasia OP, Upreti DK, Arora R, Srivastava RB (2014) Antioxidant capacities, phenolic profile and cytotoxic effects of saxicolous lichens from trans-Himalayan cold desert of Ladakh. PLoS One 9:e98696. https://doi.org/10.1371/journal.pone.0098696

Kutser T, Metsamaa L, Strombeck N, Vahtmae E (2006) Monitoring cyanobacterial blooms by satellite remote sensing. Estuar Coast Shelf Sci 67:303–312

Lange OL, Bilger W, Rimke S, Schreiber U (1989) Chlorophyll fluorescence of lichens containing green and blue- green algae during hydration by water vapor uptake and by addition of liquid water. Bot Acta 102:306–313

Láska K, Barták M, Hájek J, Prošek P, Bohuslavová O (2011) Climatic and ecological characteristics of deglaciated area of James Ross Island, Antarctica, with a special respect to vegetation cover. Czech Polar Rep 1:49–62

Letts MG, Phelan CA, Johnson DRE, Rodd SB (2008) Seasonal photosynthetic gas exchange and leaf reflectance characteristics of male and female cotton woods in a riparian woodland. Tree Physiol 28:1037–1048

Meroni M, Picchi V, Rossini M, Cogliati S, Panigada C, Nali C, Lorenzini G, Colombo R (2008) Leaf level early assessment of ozone injuries by passive fluorescence and photochemical reflectance index. Int J Remote Sens 29:5409–5422

Monteiro Estêvão DM (2015) Production of UV-B screens and changes in photosynthetic efficiency in Antarctic *Nostoc commune* colonies and a lichen *Xanthoria elegans* depend on a dose and duration of UV-B stress. Czech Polar Rep 5:55–68

Morison M, Cloutis E, Mann P (2014) Spectral unmixing of multiple lichen species and underlying substrate. Int J Remote Sens 35:478–492

Munzi S, Branquinho Ch, Cruz C, Loppi S (2012) Nitrogen tolerance in the lichen *Xanthoria parietina*: the sensitive side of a resistant species. Funct Plant Biol 40:237–243

Nakaji T, Kosugi Y, Takanashi S, Niiyama K, Noguchi S, Tani M, Oguma H, Nik AR, Kassim AR (2014) Estimation of light-use efficiency through a combinational use of the photochemical reflectance index and vapor pressure deficit in an evergreen tropical rainforest at Pasoh, Peninsular Malaysia. Remote Sens Environ 150:82–92

Naumann JC, Anderson JE, Young DR (2008) Linking physiological responses, chlorophyll fluorescence and hyperspectral imagery to detect salinity stress using the physiological reflectance index in the coastal shrub, *Myrica cerifera*. Remote Sens Environ 112:3865–3875

Nayaka S, Saxena P (2014) Physiological responses and ecological success of lichen *Stereocaulon foliolosum* and moss *Racomitrium subsecundum* growing in same habitat in Himalaya. Indian J Fundam Appl Life Sci 4:167–179

Nelson PR, Roland C, Macander MJ, McCune B (2013) Detecting continuous lichen abundance for mapping winter caribou forage at landscape spatial scales. Remote Sens Environ 137:43–54

Novis PM, Whitehead D, Gregorich ED, Hunt JE, Sparrow AD, Hopkins DW, Elberling BO, Greenfield LG (2007) Annual carbon fixation in terrestrial populations of *Nostoc commune* (Cyanobacteria) from an Antarctic dry valley is driven by temperature regime. Glob Change Biol 13:1224–1237

Orekhova A, Marečková M, Hazdrová J, Barták M (2018) The effect of upper cortex on spectral reflectance indices in Antarctic lichens during thallus dehydration. Czech Polar Rep 8(1) **(accepted, in press)**

Øvstedal DO, Lewis Smith RI (2001) Lichens of Antarctica and South Georgia. A guide to their identification and ecology. Series: studies in polar research. Cambridge University Press, Cambridge

Palumbo AD, Campi P, Modugno F, Mastrorilli M (2008) Crop water status estimated by remote sensing in formation. In: Santini A, Lamaddalena N, Severino G, Palladino M (eds) Irrigation in Mediterranean agriculture: challenges and innovation for the next decades. CIHEAM, Bari, pp 69–75, **(Options Méditerranéennes: Série A. Séminaires Méditerranéens; n. 84)**

Penuelas J, Baret F, Filella I (1995) Semi-empirical indices to assess carotenoids/chlorophyll a ratio from leaf spectral reflectance. Photosynthetica 31:221–230

Perez-Priego O, Guan J, Rossini M, Fava F, Wutzler T, Moreno G, Carvalhais N, Carrara A, Kolle O, Julitta T, Schrumpf M, Reichstein M, Migliavacca M (2015) Sun-induced chlorophyll fluorescence and photochemical reflectance index improve remote-sensing gross primary production estimates under varying nutrient availability in a typical Mediterranean savanna ecosystem. Biogeosciences 12:6351–6367

Piovano M, Guzmán G, Garbarino JA, Chamy MC (1997) *Rhizoplaca melanophthalma* a new chemical race. Biochem Syst Ecol 25:359–360

Rees WG, Tutubalina OV, Golubeva EI (2004) Reflectance spectra of subarctic lichens between 400 and 2400 nm. Remote Sens Environ 90:281–292

Ripullone F, Rivelli AR, Baraldi R, Guarini R, Guerrieri R, Magnani F, Peñuelas J, Raddi S, Borghetti M (2011) Effectiveness of the photochemical reflectance index to track photosynthetic activity over a range of forest tree species and plant water statuses. Funct Plant Biol 38:177–186

Rodriguez-Caballero E, Knerr T, Büdel B, Hill J, Weber B (2016) Cryptogamic covers control spectral vegetation indices and their seasonal variation in dryland systems. Geophys Res Abstr 18:13347 **(EGU2016-9712)**

Sand-Jensen K (2014) Ecophysiology of gelatinous *Nostoc* colonies: unprecedented slow growth and survival in resource-poor and harsh environments. Ann Bot 114:17–33

Sand-Jensen K, Jespersen TS (2012) Tolerance of the widespread cyanobacterium *Nostoc commune* to extreme temperature variations (− 269 to 105 °C), pH and salt stress. Oecologia 169:331–339

Schlensog M, Schroeter B, Sancho LG, Pintado A, Kappen L (1997) Effects of strong irradiance to the photosynthetic performance of the melt water dependent cyanobacterial lichen *Leptogium puberulum* (Collemaceae) Hue from the maritime. Antarct Bibl Lichenol 67:235–247

Shukia SP, Singh JS, Kashyap S, Giri DD, Kashyap AK (2008) Antarctic cyanobacteria as a source of phycocyanine. Indian J Mar Sci 37:446–449

Singh R, Ranjan S, Nayaka S, Pathre UV, Shirke PA (2013) Functional characteristics of a fruticose type of lichen, *Stereocaulon foliolosum* Nyl. in response to light and water stress. Acta Physiol Plant 35:1605–1615

Slavov C, Reus M, Holzwarth AR (2013) Two different mechanisms cooperate in the desiccation-induced excited state quenching In *Parmelia* Lichen. J Phys Chem B 117:11326–11336

Smith RCG, Adams J, Stephens DJ, Hick PT (1995) Forecasting wheat yield in a Mediterranean-type environment from the NOAA satellite. Aust J Agric Res 46:113–125

Stagakis S, Markos N, Sykioti O, Kyparissis A (2014) Tracking seasonal changes of leaf and canopy light use efficiency in a *Phlomis fruticosa* Mediterranean ecosystem using field measurements and multi-angular satellite hyperspectral imagery. ISPRS J Photogramm Remote Sens 97:138–151

Sun P, Wahbi S, Tsonev T, Haworth M, Liu S, Centritto M (2014) On the use of leaf spectral indices to Assess water status and photosynthetic limitations in *Olea europaea* L. during water-stress and recovery. PLoS One 9:e105165

Takaichi S, Maoka T, Mochimaru M (2009) Unique carotenoids in the terrestrial cyanobacterium *Nostoc commune* NIES-24: 2-hydroxymyxol 2′-fucoside, nostoxanthin and canthaxanthin. Curr Microbiol 59:413–419

Trnková K, Barták M (2017) Desiccation-induced changes in photochemical processes of photosynthesis and spectral reflectance in *Nostoc commune* (Cyanobacteria, Nostocales) colonies from Antarctica. Phycol Res 65:44–50

Trotter GM, Whitehead D, Pinkney EJ (2002) The photochemical reflectance index as a measure of photosynthetic light use efficiency for plants with varying foliar nitrogen contents. Int J Remote Sens 23:1207–1212

Tubuxin B, Rahimzadeh-Bajgiran P, Ginnan Y, Hosoi F, Omasa K (2015) Estimating chlorophyll content and photochemical yield of photosystem II (ΦPSII) using solar-induced chlorophyll fluorescence measurements at different growing stages of attached leaves. J Exp Bot 66:5595–5603

Van Der Veen CJ, Csatho BM (2005) Spectral characteristics of Greenland lichens. Géogr Phys Quat 59:63–73

Veerman J, Vasil'ev S, Paton GD, Ramanauskas J, Bruce D (2007) Photoprotection in the lichen *Parmelia sulcata*: The origins of desiccation-induced fluorescence quenching. Plant Physiol 145:997–1005

Wieners PC, Mudimu O, Bilger W (2012) Desiccation-induced non-radiative dissipation in isolated green lichen algae. Photosynth Res 113:239–247

Wong CYS, Gamon JA (2015) Three causes of variation in the photochemical reflectance index (PRI) in evergreen conifers. New Phytol 206:187–195

Yamano H, Chen J, Zhang Y, Tamura M (2006) Relating photosynthesis of biological soil crusts with reflectance: preliminary assessment based on a hydration experiment. Int J Remote Sens 27:5393–5399

Yamawaka H, Itoh S (2013) Dissipation of excess excitation energy by drought-induced nonphotochemical quenching in two species of drought-tolerant moss: desiccation-induced acceleration of photosystem II fluorescence decay. Biochemistry 52:4451–4459

Yebra M, Dijk AV, Leuning R, Huete A, Guerschman JP (2013) Evaluation of optical remote sensing to estimate actual evapotranspiration and canopy conductance. Remote Sens Environ 129:250–261

Zakar T, Laczko-Dobos H, Toth TN, Gombos Z (2016) Carotenoids assist in cyanobacterial photosystem II assembly and function. Front Plant Sci https://doi.org/10.3389/fpls.2016.00295 **(article 295)**

Zhang J, Rivard B, Sánchez-Azofeifa A (2005) Spectral unmixing of normalized reflectance data for the deconvolution of lichen and rock mixtures. Remote Sens Environ 95:57–66